THE JOURNAL OF BIOLOGICAL CHEMISTRY VOL. 289, NO. 52, pp. 36048–36058, December 26, 2014

Adaptor Protein GRB2 Promotes Src Tyrosine Kinase Activation and Podosomal Organization by Protein-tyrosine Phosphatase ϵ in Osteoclasts*

Received for publication, August 10, 2014, and in revised form, October 20, 2014 Published, JBC Papers in Press, November 7, 2014, DOI 10.1074/jbc.M114.603548

Einat Levy-Apter[‡], Eynat Finkelshtein[‡], Vidyasiri Vemulapalli[§], Shawn S.-C. Li[¶], Mark T. Bedford[§1], and Ari Elson[‡2]

From the [‡]Department of Molecular Genetics, The Weizmann Institute of Science, Rehovot 76100, Israel, [§]Department of Epigenetics and Molecular Carcinogenesis, The University of Texas M. D. Anderson Cancer Center, Smithville, Texas 78957, and [¶]Department of Biochemistry and the Siebens-Drake Medical Research Institute, Schulich School of Medicine and Dentistry, University of Western Ontario, London, Ontario N6A 5C1, Canada

Background: Protein-tyrosine phosphatase ϵ (cyt-PTPe) dephosphorylates and activates Src to promote osteoclast adhesion.
Results: The adaptor protein GRB2 binds phosphorylated cyt-PTPe and recruits Src, thus promoting its activation.
Conclusion: GRB2 links cyt-PTPe to Src downstream of activated integrins in osteoclasts.
Significance: GRB2-mediated recruitment may constitute a general mechanism by which cyt-PTPe activates Src and related kinases.

The non-receptor isoform of protein-tyrosine phosphatase ϵ (cyt-PTPe) supports adhesion of bone-resorbing osteoclasts by activating Src downstream of integrins. Loss of cyt-PTPe reduces Src activity in osteoclasts, reduces resorption of mineralized matrix both *in vivo* and in cell culture, and induces mild osteopetrosis in young female PTPe KO mice. Activation of Src by cyt-PTPe is dependent upon this phosphatase undergoing phosphorylation at its C-terminal Tyr-638 by partially active Src. To understand how cyt-PTPe activates Src, we screened 73 Src homology 2 (SH2) domains for binding to Tyr(P)-638 of cyt-PTPe. The SH2 domain of GRB2 bound Tyr(P)-638 of cyt-PTPe most prominently, whereas the Src SH2 domain did not bind at all, suggesting that GRB2 may link PTPe with downstream molecules. Further studies indicated that GRB2 is required for activation of Src by cyt-PTPe in osteoclast-like cells (OCLs) in culture. Overexpression of GRB2 in OCLs increased activating phosphorylation of Src at Tyr-416 and of cyt-PTPe at Tyr-638; opposite results were obtained when GRB2 expression was reduced by shRNA or by gene inactivation. Phosphorylation of cyt-PTPe at Tyr-683 and its association with GRB2 are integrin-driven processes in OCLs, and cyt-PTPe undergoes autodephosphorylation at Tyr-683, thus limiting Src activation by integrins. Reduced GRB2 expression also reduced the ability of bone marrow precursors to differentiate into OCLs and reduced the fraction of OCLs in which podosomal adhesion structures assume organization typical of active, resorbing cells. We conclude that GRB2 physically links cyt-PTPe with Src and enables cyt-PTPe to activate Src downstream of activated integrins in OCLs.

Degradation of bone is carried out by osteoclasts, which are specialized phagocytic cells derived from the hematopoietic monocyte-macrophage lineage (1–4). Osteoclasts adhere to bone tightly and secrete onto its surface a mixture of proteases and acid that degrades the organic and inorganic components of bone matrix. Adhesion to bone is key for osteoclast function; it is carried out by specific adhesion structures called podosomes, which comprise a central actin core surrounded by accessory proteins. Physical contact between an osteoclast and bone or other surfaces activates integrin molecules adjacent to the podosomal actin core and regulates the structure, organization, and turnover of podosomes (1, 5–7). We have shown previously that the non-receptor isoform of protein-tyrosine phosphatase ϵ (cyt-PTPe)[3] supports integrin signaling in osteoclasts as well as osteoclast adhesion and activity *in vivo* and *in vitro*. This is evident *in vivo* as mild osteopetrosis that is present in young female mice that genetically lack PTPe (EKO mice) and that is secondary to reduced osteoclast-mediated bone resorption *in vivo*. Osteoclast-like cells (OCLs) produced in culture from bone marrow of female EKO mice exhibit reduced resorption of mineralized matrix (8). Podosomes are typically arranged in active, resorbing osteoclasts as a large array at the cell periphery that is called a sealing zone or a sealing zone-like structure (when cells are plated on a mineralized or non-mineralized surface, respectively). Less active cells exhibit podosomes arranged in smaller clusters or dispersed at random throughout the cell (1). OCLs from young female EKO mice exhibit a marked reduction in the fraction of cells exhibiting a

* This work was supported by the Israel Science Foundation and by the Kekst Family Institute for Medical Genetics and the David and Fella Shapell Family Center for Genetic Disorders Research, both of the Weizmann Institute (to A. E.).
[1] Directs the Protein Array Core, which is supported by Cancer Prevention Research Institute of Texas Grant RP130432 and by the Centre for Environmental and Molecular Carcinogenesis at M. D. Anderson.
[2] To whom correspondence should be addressed. Tel.: 972-8-934-2331; Fax: 972-8-934-4108; E-mail: ari.elson@weizmann.ac.il.

[3] The abbreviations used are: cyt-PTPe, non-receptor isoform of protein-tyrosine phosphatase ϵ; EKO, PTPe knock-out; OCL, osteoclast-like cell; PTP, protein-tyrosine phosphatase; PTPe, protein-tyrosine phosphatase ϵ; RPTPe, receptor-type form of PTPe; RPTPa, receptor-type PTPα; SH2, Src homology 2; SH3, Src homology 3; SZL, sealing zone-like structure; BES, 2-[bis(2-hydroxyethyl)amino]ethanesulfonic acid; M-CSF, macrophage colony-stimulating factor; RANKL, receptor activator of nuclear factor κB ligand; N-SH3, N-terminal SH3; C-SH3, C-terminal SH3; GRB2, growth factor receptor-bound protein 2.

sealing zonelike structure (SZL) in agreement with their reduced ability to resorb mineralized matrix (8, 9).

At the molecular level, cyt-PTPe helps activate the Src tyrosine kinase downstream of integrins in osteoclasts. We have shown that following integrin activation cyt-PTPe undergoes phosphorylation by partially active Src at its C-terminal Tyr-638. Phosphorylated cyt-PTPe associates with Src and Pyk2 after which cyt-PTPe dephosphorylates Src at its inhibitory Tyr-527 and fully activates the kinase. Consequently, downstream events that are required for resorption, including activation of Rac and inhibition of Rho, are set in motion (9). Lack of cyt-PTPe in osteoclasts results in reduced Src activity and alters podosomal structure, function, and stability in EKO OCLs; these parameters can be rescued when exogenous cyt-PTPe is expressed in these cells. Phosphorylation of cyt-PTPe at Tyr-638 is critical in this aspect because the non-phosphorylatable mutant Y638F cyt-PTPe cannot rescue Src activity in EKO osteoclasts (9). The central role of C-terminal phosphorylation of PTPe is evident also in other, non-bone settings. Phosphorylation of the receptor-type form of PTPe (RPTPe) at the analogous residue Tyr-695 is required for activation of Src downstream of ErbB2/Neu in mouse mammary tumors (10, 11) and for inhibition of JAK2 downstream of the activated leptin receptor in hypothalamic neurons (12). C-terminal phosphorylation of cyt-PTPe by the activated EGF receptor drives the phosphatase to associate with microtubules and inhibits its activity (13). Nonetheless, the molecular details of how cyt-PTPe associates with Src and activates it remain unclear.

The closely related receptor-type PTPα (RPTPa) possesses a C-terminal tyrosine, Tyr-789, which is embedded in a sequence similar to that of Tyr-638 of cyt-PTPe. Like cyt-PTPe, RPTPa can undergo phosphorylation at Tyr-789 and activate Src. Two alternative models have been proposed to explain activation of Src by RPTPa. The direct phosphodisplacement model suggests that Tyr(P)-789 of RPTPa directly binds the SH2 domain of Src, thus displacing Tyr(P)-527 of the kinase and inducing an open, active conformation of the kinase. RPTPa then dephosphorylates Src at Tyr-527, thus preventing this residue from binding the Src SH2 domain and returning the kinase to its inhibited state (14). Studies of cells undergoing mitosis suggest that the adaptor molecule GRB2, which also binds RPTPa at Tyr(P)-789 (15–18), competes against Src for binding RPTPa and is thus an inhibitor of Src activation by the phosphatase (19). An alternative model proposes that RPTPa associates with Src indirectly via the adaptor molecule GRB2 (20), which can bind RPTPa via the GRB2 SH2 domain and one of its SH3 domains. Here too binding depends on RPTPa phosphorylation at Tyr-789. GRB2 recruits the Src·focal adhesion kinase complex to RPTPa, thus allowing these kinases to phosphorylate RPTPa and enabling the phosphatase to recruit the BCAR3·Cas complex and promote cell migration (20, 21). The distinction between both models with respect to GRB2 function is significant. In the phosphodisplacement model, GRB2 competes against the RPTPa-Src association and inhibits activation of Src, whereas in the indirect model, GRB2 facilitates the association and promotes signaling. In this study, we examined the molecular mechanism by which cyt-PTPe activates Src in osteoclasts and conclude that it occurs by an indirect, GRB2 binding mechanism.

EXPERIMENTAL PROCEDURES

Antibodies

The following polyclonal antibodies were used: anti-PTPe (22); polyclonal anti-phospho-PTPe (Tyr-638 in cyt-PTPe is equivalent to Tyr-695 in RPTPe (11)); anti-Tyr(P)-416 Src, anti-Src, and anti-Tyr(P)-402 Pyk2 (Cell Signaling Technology, Danvers, MA); and anti-GRB2 (c-23), anti-Src2, and anti-HA (Santa Cruz Biotechnology, Inc., Dallas, TX). Monoclonal antibodies used included anti-v-Src (clone 327; Calbiochem); anti-α-tubulin (clone DM1A), anti-actin (clone AC-40), and anti-FLAG M2 (Sigma-Aldrich); anti-GRB2 and anti-Pyk2 (clones 81 and 11, respectively; BD Transduction Laboratories); anti-HA (clone 16B12; Covance, Princeton, NJ); anti-glutathione *S*-transferase (GST) (clone 8-326; Merck Millipore, Darmstadt, Germany); and anti-Tyr(P) (clone pY99; Santa Cruz Biotechnology, Inc.). Horseradish peroxidase-conjugated secondary antibodies (goat anti-mouse or goat anti-rabbit) for protein blotting were purchased from Jackson ImmunoResearch Laboratories (West Grove, PA).

Protein Array Experiments

The cloning of the human SH2 domain library has been described previously (23). All SH2 domains were expressed as GST fusions in *Escherichia coli* and purified on glutathione-Sepharose beads. The recombinant SH2 domains were arrayed onto nitrocellulose-coated glass slides (Oncyte®Avid slides, Grace Bio-Labs, Bend, OR) using a pin arrayer as described previously (24). A list of the SH2 domains on this array is given in Fig. 1. The fluorescent labeling of the biotinylated peptide probe and slide binding have also been described previously (24). Fluorescent signal was detected using a GeneTAC™ LSIV scanner (Genomic Solutions).

Mice

Gene-targeted mice lacking PTPe (EKO mice) (25) were used in the 129 SvEv genetic background. *Grb2* floxed conditional knock-out mice (26) were a generous gift of Prof. Tony Pawson, Samuel Lunenfeld Research Institute. Inactivation of *Grb2* floxed alleles in osteoclasts was achieved by crossing *Grb2* Flox+/− mice with mice expressing Cre under direction of the cathepsin K promoter (27), a generous gift from Prof. Shigeaki Kato, University of Tokyo. Mouse studies were approved by Weizmann Institute's Animal Ethics committee (Institutional Animal Care and Use Committee) and were performed in accordance with Israeli Law and Weizmann Institute regulations.

Cell Culture

Human kidney 293T cells were grown in DMEM as described (11). Transient transfection of 293T cells was by BES-calcium phosphate technique (28). Cells were analyzed 24–48 h following transfection. For primary osteoclasts, bone marrow was collected from femora, tibiae, and humeri of 6–8-week-old mice as described (9). Cells were cultured in complete OCL medium (α-minimum Eagle's medium (Sigma-Aldrich) containing 10%

fetal calf serum (Biological Industries, Beit Haemek, Israel), 2 mM glutamine, 50 units/ml penicillin, and 50 g/ml streptomycin) supplemented with 20 ng/ml M-CSF (Peprotech, Rocky Hill, NJ) and 20 ng/ml RANKL (R&D Systems, Minneapolis, MN). Bone marrow cells were plated at a density of 5–7 $\times$ 10^6 cells/well of a 6-well plate or 1 $\times$ 10^6 cells/well of a 24-well plate and incubated at 37 °C in 5% CO_2 for 5 days (day of seeding is counted as day 0) with daily changes of medium. When needed, cells were fixed and stained for tartrate-resistant acid phosphatase activity using a commercial kit (Sigma-Aldrich).

Viral Infection of OCLs

Adenoviral Infection (for Expression of Exogenous Proteins)—Primary bone marrow cells were grown for 2 days in OCL medium supplemented with M-CSF and RANKL. On day 2 postseeding, medium was replaced with OCL medium containing M-CSF, RANKL, and adenoviruses (in the form of medium from 293 cells used to amplify the virus; 200–350 μl/well of 6-well plate or 50–100 μl/well of a 24-well plate). Following overnight incubation, the medium was replaced with OCL medium/cytokines; cells were then fed daily with similar OCL medium until collected. Adenoviruses were produced with the AdEasy XL adenoviral vector system (Stratagene, Agilent Technologies, Inc., Santa Clara, CA) and amplified using 293AD cells.

Lentiviral Infection (for shRNA Expression)—Mouse lentiviral particles were produced as described (29) using *Grb2* or non-targeting shRNAs purchased from Open Biosystems. For infection, bone marrow cells were seeded in 6-well plates in complete OCL medium supplemented with M-CSF and RANKL as described above. On day 3 of differentiation, medium was replaced with medium harvested from 293T cells expressing lentiviruses (3–4 ml/well of a 6-well plate) supplemented with 8 μg/ml Polybrene. The cells were then centrifuged (with the lentivirus-containing medium) at 500 $\times$ *g* at 30 °C for 1.5 h. Virus-containing medium was then removed, and the cells were fed daily with complete OCL medium containing M-CSF and RANKL until collected. In some cases, OCLs were infected sequentially with lentiviruses on day 2 followed by adenoviral infection the following day as described.

Replating of Osteoclasts

Primary bone marrow cells were prepared and grown for 4 days in OCL medium supplemented with M-CSF and RANKL. On their 4th day of differentiation, cells were incubated for 4 h in OCL medium containing 1% serum and no cytokines (adherent cells). Cells were then detached by a short treatment with 10 mM EDTA, suspended in DMEM containing 20 mM HEPES and 1 mg/ml bovine serum albumin, and incubated at 37 °C for 1 h with gentle rotation (suspended cells). Cells were then replated on plates precoated with 20 μg/ml fibronectin (Sigma-Aldrich), and readherent cells were analyzed 30 min after replating.

Analysis of Podosomal Organization in OCLs

Primary bone marrow cells were prepared as above and seeded on glass coverslips (Menzel-Glaser, Braunschweig, Germany) or in chambers (Ibidi GmbH, Munich, Germany) in OCL medium supplemented with M-CSF and RANKL. On day 2 or 3 of differentiation, cells were infected with adenoviruses or lentiviruses as described above. After 4 days of differentiation, OCLs were fixed in paraformaldehyde and stained with phalloidin to visualize actin as described (30). Images were collected with an inverted microscope (Olympus Corp., Tokyo, Japan). Images were acquired using CellSense Dimension software (Olympus Corp.). Cells were analyzed visually and scored as displaying a complete podosomal SZL (fully polarized), partial podosomal belt and rings (partially polarized), or podosomes arranged in small clusters or at random (non-polarized). Analyses were performed in a manner blinded to the genotypes of the cells.

Preparation of Cell Lysates, Immunoprecipitation, and Protein Blotting

Cells were washed with ice-cold PBS and lysed in Buffer A (50 mM Tris-Cl, pH 8, 150 mM NaCl, 1% Nonidet P-40) and protease inhibitors (1 mM 4-(2-aminoethyl)benzenesulfonyl fluoride, 40 μM bestatin, 15 μM E-64, 20 μM leupeptin, 15 μM pepstatin; Sigma); 0.5 mM sodium pervanadate was included when tyrosine phosphorylation of proteins was evaluated. Protein concentration was determined by the Bio-Rad protein assay with bovine serum albumin as a standard. In FLAG precipitation studies, cellular proteins (0.5–1.5 mg) were incubated with anti-FLAG M2 affinity beads for 3 h at 4 °C. Immunoprecipitates were washed in Buffer A, and the proteins were eluted using FLAG peptide (Sigma) or by boiling in 100 °C for 3 min in SDS sample buffer. In GRB2 precipitation, GRB2-conjugated beads (Santa Cruz Biotechnology, Inc.) were used. For other precipitations, protein G beads were incubated with the specified antibody for 2 h, washed, and then incubated with the lysate for an additional 3 h. For protein blotting, 25–30 μg of lysate proteins were subjected to 10% SDS-PAGE and transferred onto a nitrocellulose membrane (Protran Whatman, GE Healthcare). The membranes were blocked in 5% milk and 0.05% Tween 20 for 1 h and incubated with primary antibody at 4 °C overnight followed by probing with secondary antibodies coupled with HRP. Bands were detected by ECL (Biological Industries).

Bacterial Expression and GST Pulldown

GST-GRB2 fusion constructs were generous gifts from Prof. Thomas M. Roberts, Dana-Farber Cancer Institute (full-length wild-type GRB2 and isolated N-terminal SH3 (N-SH3), SH2, and C-terminal SH3 (C-SH3) domains) and Prof. Jan Sap, University of Paris Diderot (full-length wild-type GRB2 and the GRB2 point mutants P49L, R86K, and G203R). GST fusion constructs were grown in BL26 bacteria, purified, and used in pulldown studies as described (31).

In Vitro Dephosphorylation of cyt-PTPe

FLAG- or HA-tagged cyt-PTPe was expressed in 293T cells. FLAG-tagged cyt-PTPe was precipitated in the absence of PTP inhibitors to ensure its activity and eluted from the precipitating beads with FLAG peptide as described (13). HA-tagged cyt-PTPe was precipitated from cells treated with sodium pervanadate to ensure its phosphorylation (which occurs only at Tyr-638) and its inactivity. Soluble FLAG-cyt-

PTPe was added to bead-bound HA-cyt-PTPe and incubated at 37 °C for 30 min in reaction buffer after which the beads were washed from FLAG-cyt-PTPe and HA-cyt-PTPe was eluted by boiling and then analyzed by SDS-PAGE and blotting as indicated. Control experiments exposed bead-bound HA-cyt-PTPe to material eluted from FLAG beads incubated with lysates of mock-transfected 293T cells.

Statistics

Results were analyzed by the two-tailed Student's *t* test. Significant results are $p < 0.05$.

RESULTS

Tyr(P)-638 cyt-PTPe Binds the SH2 Domain of GRB2 but Not of Src—Phosphorylation of cyt-PTPe at Tyr-638 in OCLs is required for cyt-PTPe to bind the Src·Pyk2 complex, to activate Src, and to regulate the lifespan of podosomal adhesion structures (9). Phosphorylation at Tyr-638 has not been shown to affect the catalytic properties of cyt-PTPe (11); hence it most likely affects binding of the phosphatase to other molecules. Prime candidates for binding Tyr(P)-638 cyt-PTPe are SH2 domain-containing proteins, such as the adaptor protein GRB2 (31). To search for additional molecules that bind Tyr(P)-638 and may mediate its function in OCLs, we used a synthetic peptide containing the 10 C-terminal amino acids of cyt-PTPe, including Tyr(P)-638, to screen an array of 73 distinct SH2 domains fused to GST (Fig. 1, *A–C*). The phosphopeptide bound the SH2 domain of GRB2 very prominently; interestingly, all the other SH2 domains assayed did not bind the peptide or did so very weakly. In particular, the SH2 domain of Src did not bind the peptide at all (Fig. 1*A*). As expected, the control non-phosphorylated peptide did not bind the SH2 domain of GRB2 (not shown). To confirm these results, we used GST fusion molecules of the SH2 domains of GRB2 or Src to pull down full-length cyt-PTPe from cell lysates. Cells were treated with pervanadate prior to lysis to ensure phosphorylation of cyt-PTPe at Tyr-638. As expected, WT cyt-PTPe was pulled down by the SH2 domain of GRB2 but not of Src (Fig. 1*D*). In agreement with prior studies (31), this association was dependent on Tyr(P)-638 because the non-phosphorylatable Y638F cyt-PTPe mutant did not bind the GRB2 SH2 domain (Fig. 1*D*). We conclude that Tyr(P)-638 of cyt-PTPe binds the SH2 domain of GRB2 to a significantly greater extent than the Src SH2 domain. The prominent binding of the GRB2 SH2 domain to cyt-PTPe suggested that GRB2 might mediate its activation of Src.

GRB2 Promotes Phosphorylation of cyt-PTPe and Activation of Src and Pyk2 in Osteoclasts—To examine the possible role of GRB2 in activation of Src by cyt-PTPe, we expressed GRB2 in OCLs. Cyt-PTPe, Src, and Pyk2 are all phosphorylated in adherent OCLs at positions Tyr-638, Tyr-416, and Tyr-402, respectively. Expression of exogenous GRB2 in OCLs increased phosphorylation of all three proteins, indicating that added GRB2 supports both phosphorylation of cyt-PTPe and activation of the downstream kinases Src and Pyk2 (Fig. 2*A*). In separate studies, we expressed cyt-PTPe and GRB2 in 293 cells (Fig. 2*B*). Although weak basal phosphorylation of cyt-PTPe was detected in these cells, treatment of the cells with the PTP inhibitor sodium pervanadate or expression of GRB2 in otherwise untreated cells increased phosphorylation of cyt-PTPe at Tyr-638. Combining both treatments increased PTPe phosphorylation even further (Fig. 2*B*). This latter result is consistent with GRB2 recruiting a kinase to phosphorylate cyt-PTPe molecules, thus increasing overall phosphorylation of this PTP beyond what can be expected due to PTP inhibition alone. In agreement, down-regulation of GRB2 expression in OCLs yielded opposite results (Fig. 3). Separate lentivirus-mediated expression of two distinct shRNAs targeting *Grb2* each reduced GRB2 protein levels by 50%, correlating with significantly reduced levels of Tyr(P)-638 cyt-PTPe and Tyr(P)-416 Src in these cells (Fig. 3*A*). Expression of exogenous shRNA-resistant GRB2 in OCLs in which GRB2 was knocked down rescued phosphorylation of cyt-PTPe, Src, and Pyk2 (Fig. 3*B*), confirming that the reduced phosphorylation seen in Fig. 3*A* was due to reduced expression of GRB2.

Although the above studies establish a correlation between expression levels of GRB2 and phosphorylation of cyt-PTPe and Src, they do not indicate whether GRB2 is required for activation of Src by cyt-PTPe. To address this issue, we examined OCLs from EKO mice. Phosphorylation of Src at Tyr-416 is very low in EKO OCLs and was significantly increased when exogenous cyt-PTPe was expressed in these cells (Ref. 9 and Fig. 3*C*). However, expression of exogenous cyt-PTPe in EKO OCLs did not increase Src phosphorylation when GRB2 was knocked down (Fig. 3*C*), indicating that GRB2 is required for cyt-PTPe to activate Src and to induce its phosphorylation at Tyr-416. We note that phosphorylation of cyt-PTPe at Tyr-638 is critical for activation of Src as the non-phosphorylatable Y638F cyt-PTPe cannot activate Src in osteoclasts (9).

Cyt-PTPe and GRB2 Associate in an Adhesion-dependent Manner in OCLs—Our prior studies indicated that Src and cyt-PTPe can physically associate in OCLs in a manner dependent on phosphorylation of cyt-PTPe at Tyr-638 (9). Because GRB2 binds cyt-PTPe at this residue (31) and affects its phosphorylation (Figs. 2 and 3), we examined whether GRB2 is associated with the cyt-PTPe·Src complex. These studies were performed with endogenous proteins at their levels of expression in OCLs. Indeed, GRB2 co-precipitated together with cyt-PTPe and Src in freely growing, adherent OCLs (Fig. 4, *A* and *B*). Importantly, co-precipitation of cyt-PTPe with GRB2 increased dramatically when OCLs were lifted from plates and allowed to readhere to plates coated with the $\alpha v\beta 3$ integrin ligand fibronectin (Fig. 4*C*). Strong co-precipitation observed in readherent cells is most likely the result of widespread and synchronized integrin activation in the entire cell population following replating. This point is further underscored by the finding that phosphorylation of cyt-PTPe at Tyr-638, which is required for binding of GRB2 (Fig. 1 and Ref. 31) and for activation of Src (9, 11), was induced in readherent OCLs (Fig. 4*D*). As expected, phosphorylation of Src at Tyr-416 followed the same pattern (Fig. 4*D*). We conclude that GRB2 participates in the association between cyt-PTPe and Src in OCLs and that the association with cyt-PTPe is promoted by adhesion of OCLs. We note that Pyk2 binds cyt-PTPe in OCLs in a Tyr(P)-638 cyt-PTPe-dependent manner (9) and associated with GRB2 in OCLs (Fig. 4*A*), sug-

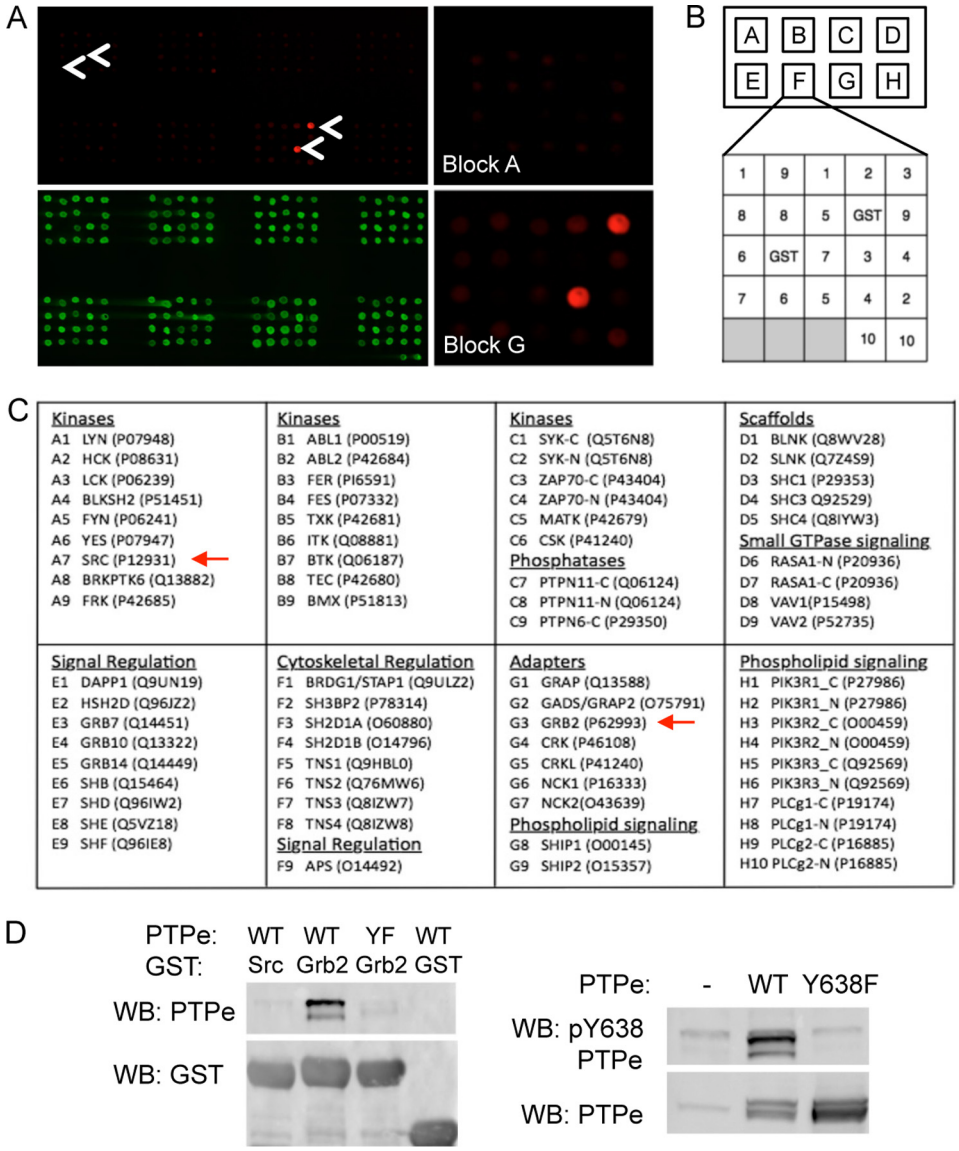

FIGURE 1. **Tyr(P)-638 of cyt-PTPe binds the SH2 domain of GRB2 but not of Src.** *A*, *top left*, array hybridized with phosphorylated PTPe probe (DIFSDpYANFK where pY is phosphotyrosine; *red*). *Arrowheads* mark the location of twin spots for Src (*Block A*, no spots) and GRB2 (*Block G*, two *red* spots). *Bottom left*, same array probed with anti-GFP antibodies to visualize all individual samples (*green*). *Right*, magnified views of Blocks A and G hybridized with the phosphopeptide. *B*, organization of samples in the array. The array is composed of eight blocks that contain up to 10 samples each; each sample is spotted in duplicate in a unique pattern in a 5 × 5 square (*inset*). *C*, list of the 73 individual GST-SH2 fusion proteins in the array. Src and GRB2 are marked by *red arrows*. *D*, *left*, pulldown of full-length cyt-PTPe protein from pervanadate-treated 293 cell lysates with GST fusion proteins of the SH2 domains of GRB2 or Src. *Right*, protein blot showing phosphorylation of cyt-PTPe at Tyr-638 in the various samples used in the pulldown. *WB*, Western blot.

gesting that this kinase may also be associated with the cyt-PTPe·GRB2·Src complex. This issue requires further studies.

Binding of GRB2 to Src Does Not Require cyt-PTPe—To understand how GRB2 binds Src in OCLs, we examined association between individual domains of GRB2 and Src. A GST fusion protein of full-length GRB2 pulled down Src from lysates of WT OCLs (Fig. 5*A*). GST fusions of the isolated SH2 or N-SH3 domains of GRB2 pulled down Src, possibly to a lesser extent than did full-length GRB2. The C-SH3 domain of GRB2 did not pull down Src at all (Fig. 5*A*). This result suggests that GRB2 binds Src using the SH2 and N-terminal SH3 domains. GST fusion proteins of full-length GRB2 in which inactivating point mutations were introduced individually into the N-SH3 (P49L), SH2 (R86K), and C-SH3 (G203R) domains (32, 33) all pulled down Src from OCL lysates (Fig. 5*B*). This suggests that in the context of the full GRB2 molecule inactivation of binding by a single domain of GRB2 is insufficient to prevent binding to Src. The results also confirm that GRB2 binds cyt-PTPe only via its SH2 domain as shown previously (31). Specifically, of the isolated GRB2 domains, only the SH2 domain bound cyt-PTPe (Fig. 5*A*), whereas inactivating the SH2 domain in full-length GRB2 was sufficient to abrogate the GRB2-cyt-PTPe association (Fig. 5*B*). Binding of GRB2 to Src occurs independently of cyt-PTPe as GRB2 co-immunoprecipitated with Src and Pyk2 equally well in OCLs prepared from wild-type and EKO mice (Fig. 5*C*).

Reduced Expression of GRB2 Reduces OCL Differentiation and Affects Podosomal Organization in Osteoclasts—Absence of cyt-PTPe and reduced activity of Src in OCLs significantly reduce the fraction of OCLs that organize their podosomes into

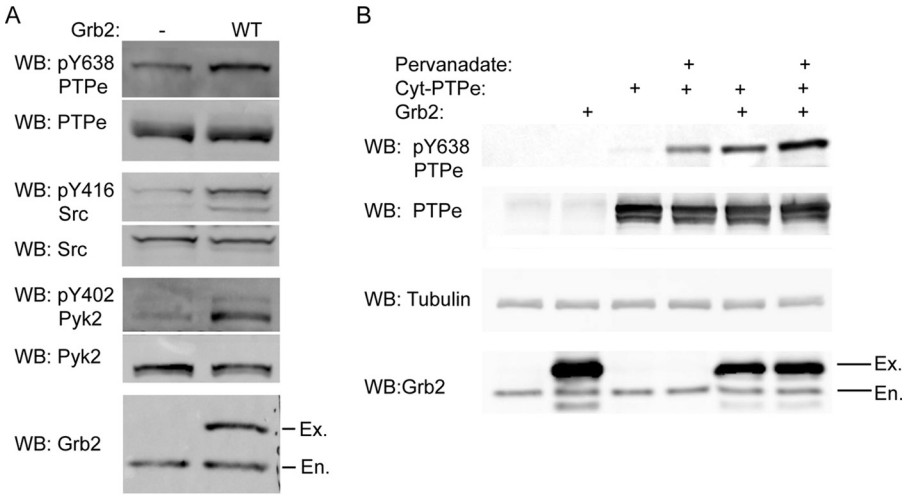

FIGURE 2. **Overexpression of GRB2 increases phosphorylation of cyt-PTPe, Src, and Pyk2.** *A*, GRB2 was overexpressed in primary OCLs from WT mice; shown is phosphorylation of cyt-PTPe, Src, and Pyk2. *B*, GRB2 overexpression in 293T cells. Expressing GRB2 and treating cells with pervanadate increased Tyr(P)-638 cyt-PTPe levels additively. *Ex*. and *En*., exogenous and endogenous GRB2, respectively; *WB*, Western blot.

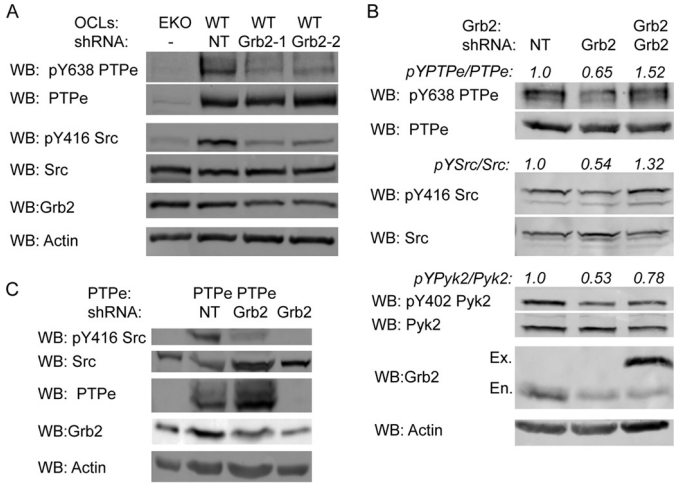

FIGURE 3. **Knockdown of GRB2 decreases phosphorylation of cyt-PTPe, Src, and Pyk2.** *A*, inhibition of GRB2 in primary WT OCLs reduces phosphorylation of cyt-PTPe and Src at Tyr-638 and Tyr-416, respectively. *NT*, non-targeting, control shRNA; *Grb2-1* and *Grb2-2*, two distinct targeting shRNAs. *B*, restoration of GRB2 expression in primary WT OCLs in the presence of *Grb2* shRNA (*Grb2-1*) rescues phosphorylation of cyt-PTPe, Src, and Pyk2. *C*, Cyt-PTPe requires GRB2 to induce phosphorylation of Src at Tyr-416. Primary OCLs from EKO mice exhibit reduced Tyr(P)-416 Src levels, which are rescued upon cyt-PTPe expression. Inhibition of GRB2 by shRNA prevents cyt-PTPe from rescuing Src phosphorylation. *NT*, non-targeting shRNA; *Grb2*, shRNA against *Grb2*; *Ex*. and *En*., exogenous and endogenous GRB2, respectively; *WB*, Western blot.

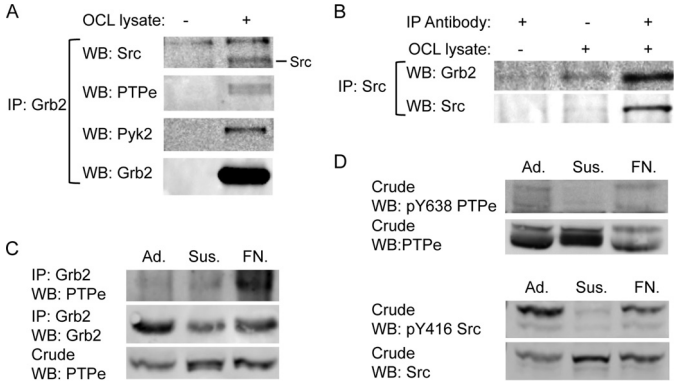

FIGURE 4. **GRB2 associates with cyt-PTPe and with Src in OCLs.** *A*, Src, cyt-PTPe, and Pyk2 co-precipitate with GRB2 from adherent primary OCLs of WT mice. *B*, GRB2 co-precipitates with Src from adherent primary WT OCLs. *C*, cyt-PTPe co-precipitates with GRB2 strongly in WT OCLs that were lifted from plates, held for 30 min in suspension, and then replated for 30 min on fibronectin-coated plates (*FN*.). *Ad*., adherent OCLs; *Sus*., OCLs held in suspension for 30 min. *D*, integrin activation induces phosphorylation of cyt-PTPe and Src in primary WT OCLs. Both proteins are phosphorylated in adherent (*Ad*.) cells and in cells reattached to fibronectin-coated surface (*FN*.) but not in cells held in suspension (*Sus*.). *IP*, immunoprecipitation; *WB*, Western blot.

a sealing zone-like structure characteristic of mature, active OCLs (9, 30). Because reduced expression of GRB2 inhibited activation of Src by cyt-PTPe (Fig. 3, *A* and *B*), we asked whether reduced GRB2 levels would also affect production and growth of OCLs and organization of their podosomal adhesion structures. As can be seen in Fig. 6*A*, shRNA-mediated inhibition of GRB2 expression resulted in OCLs that appeared healthy but grew somewhat sparser and included a larger number of smaller OCLs than WT cultures. In agreement, OCLs expressing reduced levels of GRB2 covered a smaller fraction of the area of the plates on which they were grown (Fig. 6*B*). Decreasing GRB2 protein levels by about 50% shifted podosome organization patterns in these cells, reducing significantly the fraction of OCLs that display an SZL and increasing the fraction of cells in which podosomes are less well organized (Fig. 6*C*). Importantly, this shift was partially rescued by expression of exogenous GRB2, confirming that the disruption of podosomal organization in these cells was indeed caused by reduced GRB2 expression (Fig. 6*C*). Incomplete rescue of podosomal organization by expression of exogenous GRB2 may arise from the need to use both lentiviruses and adenoviruses in the same set of delicate OCLs in this study.

GRB2 is a major participant in various signaling events in cells. Although our results indicate that GRB2 helps link Src with cyt-PTPe in OCLs, this is most likely not its only function in these cells. To examine this issue, we compared the extent of podosomal disruption caused by reduced GRB2 expression with the disruption caused by absence of cyt-PTPe in OCLs. Consistent with our previous studies (9), cultures of OCLs from mice lacking cyt-PTPe contained fewer OCLs displaying a well organized SZL (Fig. 6*D*). Reducing GRB2 expression by about

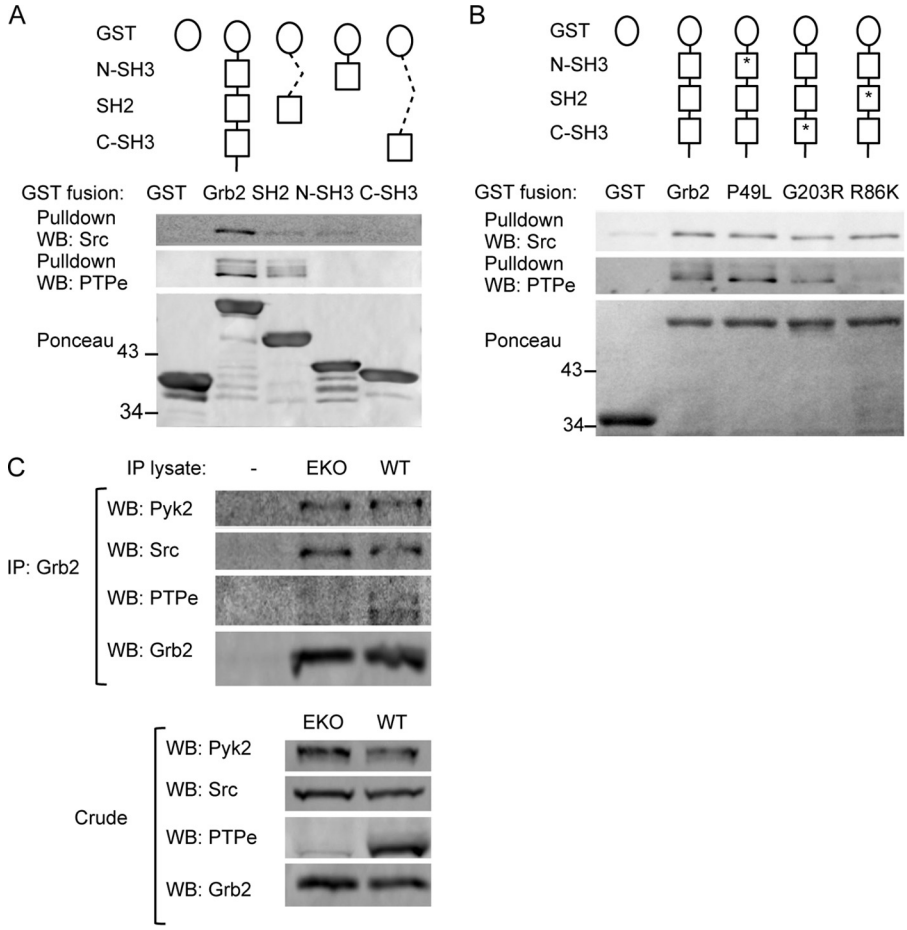

FIGURE 5. **Distinct domains of GRB2 bind Src and cyt-PTPe.** *A*, GST fusion proteins of full-length GRB2 or of its isolated SH2, N-SH3, and C-SH3 domains were used to pull down Src and cyt-PTPe from lysates of primary WT osteoclasts (*top two panels*). *Dashed lines* in the schematic structure of the GST proteins used indicate deleted sequences. *Bottom panel*, Ponceau S staining to document GST fusion proteins used. *B*, similar to *A* except that pulldown was performed using GST fusions of full-length GRB2 molecules in which binding by the N-SH3, C-SH3, or SH2 domain was abrogated by specific point mutations (P49L, G203R, R86K, respectively; marked as *asterisks* in the schematic drawing above the blot). *C*, GRB2 binds Src independently of cyt-PTPe. Src and Pyk2 co-precipitate with GRB2 in OCLs from EKO and from WT mice. Cyt-PTPe is present in and precipitates only from WT cells. *IP*, immunoprecipitation; *WB*, Western blot.

50% in OCLs that express endogenous cyt-PTPe resulted in a similar shift in podosomal organization. Combining both effects by reducing GRB2 expression in EKO OCLs resulted in a more severe podosomal disorganization phenotype and in more significantly reduced phosphorylation of Src at Tyr-416 (Fig. 6*D*). These last results suggest that GRB2 affects podosomal organization and Src phosphorylation also independently of cyt-PTPe.

shRNA studies described above down-regulated GRB2 protein levels by ~50%. To verify these results in a second experimental system, we examined mice in which the *Grb2* gene was inactivated genetically. Because whole-body *Grb2* knock-out mice display an embryonic lethal phenotype, we examined OCLs derived from mice carrying a conditional floxed allele of *Grb2* that had been inactivated in OCLs by Cre driven by the cathepsin K promoter (26, 27). Strong expression of Cre by the cathepsin K promoter is detected in OCLs differentiated *in vitro* from bone marrow cells starting at day 3 of culture (27); hence we examined OCLs that had been cultured for 3–4 days. As shRNA reduced expression of GRB2 by about 50% in our studies (Fig. 3), we examined OCLs derived from mice that carried one copy of the floxed *Grb2* allele and in which Cre-mediated recombination reduced GRB2 levels by a similar extent (Fig. 7*A*). As was seen in OCLs in which GRB2 was knocked down, inactivation of one *Grb2* allele resulted in reduced levels of Tyr(P)-416 Src and Tyr(P)-638 cyt-PTPe (Fig. 7*B*) and in sparser cultures that covered a smaller fraction of the tissue culture dish relative to control cells (Fig. 7, *C* and *D*). Podosomal organization in these cells was also disrupted: loss of one *Grb2* allele resulted in significantly fewer OCLs containing a well organized SZL (Fig. 7*E*). OCLs produced from mice expressing the cathepsin K-Cre transgene and carrying two wild-type, non-floxed alleles of *Grb2* did not display reduced GRB2 protein expression or reduced phosphorylation of cyt-PTPe or Src (Fig. 7, *A* and *B*). The growth and podosomal organizations of these cells were also unchanged relative to controls (not shown), indicating that the phenotypes observed in *Grb2* floxed mice were caused by Cre-mediated disruption of one *Grb2* allele and not by the mere presence of the cathepsin K-Cre transgene.

The important role of phosphorylation of cyt-PTPe at Tyr-638 in binding GRB2 and in activating Src suggests that dephosphorylation of this residue, possibly by cyt-PTPe itself, might inhibit activation of Src by cyt-PTPe. To determine whether

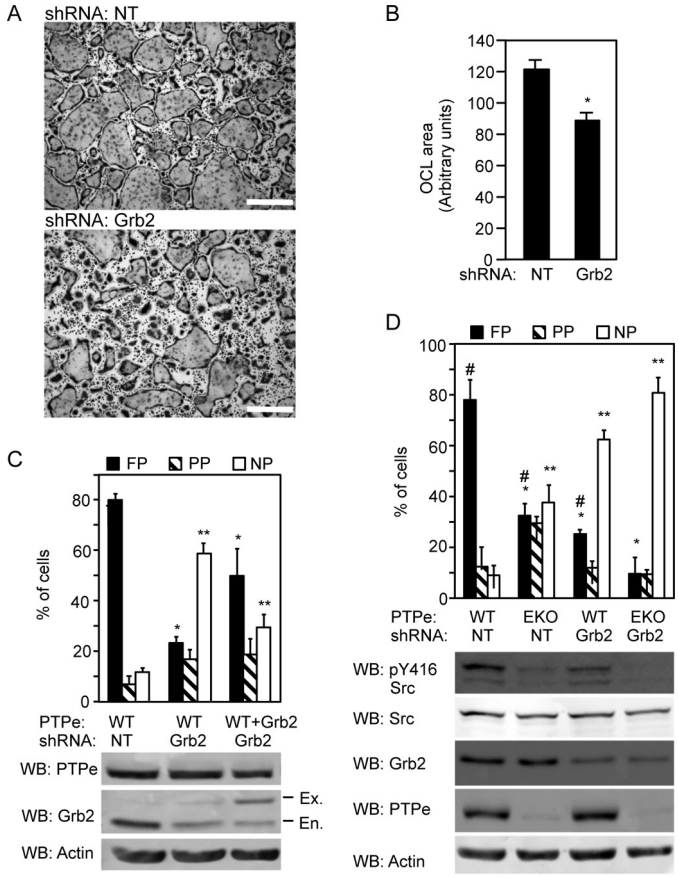

FIGURE 6. **Knockdown of GRB2 in primary OCLs disrupts cell growth and podosomal organization.** *A*, primary WT OCLs were treated with non-targeting shRNA (*NT*) or *Grb2* shRNA. Shown are pictures of growing OCLs stained for tartrate-resistant acid phosphatase. *Scale bars*, 200 μm. *B*, bar diagram comparing the area of the plate covered by OCLs in OCLs treated with non-targeting shRNA *versus Grb2* shRNA. *, $p = 0.00075$, 9–10 fields per genotype in two separate experiments. *C*, percentage of WT OCLs whose podosomes are organized in SZLs (fully polarized (*FP*)), in small rings or associations (partially polarized (*PP*)), or at random (non-polarized (*NP*)). Compared are OCLs treated with non-targeting shRNA (*NT*) and shRNA against *Grb2* and cells treated with *Grb2* shRNA in which GRB2 is re-expressed. Also shown is expression of cyt-PTPe and GRB2 in the cells. *Ex.* and *En.*, external and endogenous GRB2, respectively; *WB*, Western blot. *D*, absence of cyt-PTPe and knockdown of GRB2 affect podosomal organization and Src Tyr(P)-416 phosphorylation in an additive manner. Podosomal organization (*top*) was analyzed as in *C* in OCLs from WT or EKO mice that had been treated with non-targeting (*NT*) or *Grb2* shRNA. Tyr(P)-416 Src levels were analyzed by protein blotting. In *C* and *D*, * represents $p < 0.025$ and ** represents $p < 0.0038$ by *t* test relative to fully polarized and non-polarized bars of WT/non-targeting shRNA, respectively. #, $p < 0.013$ by *t* test relative to EKO/GRB2. 70–240 cells were analyzed per genotype/treatment. *Error bars* represent S.E.

cyt-PTPe can undergo autodephosphorylation at Tyr-638, we examined the ability of active cyt-PTPe molecules to dephosphorylate in *trans* inactive Tyr(P)-638 cyt-PTPe. This approach was required because we could not isolate cyt-PTPe molecules that are simultaneously active and phosphorylated at Tyr-638, a finding itself consistent with cyt-PTPe autodephosphorylation. HA-tagged Tyr(P)-638 cyt-PTPe was purified from cells treated with sodium pervanadate prior to lysis; this treatment irreversibly inactivates the phosphatase and induces its phosphorylation at Tyr-638. FLAG-tagged, active unphosphorylated cyt-PTPe was purified from cells not treated with pervanadate. As seen in Fig. 8*A*, incubating inactive Tyr(P)-638 HA-cyt-PTPe with active FLAG-cyt-PTPe reduced phosphorylation of HA-cyt-PTPe in a manner proportional to the amount of FLAG-cyt-PTPe added. Phosphorylation of HA-cyt-PTPe was not reduced in control reactions in which no FLAG-cyt-PTPe was added, confirming that the dephosphorylation observed was performed by FLAG-cyt-PTPe. These results indicate that cyt-PTPe can undergo *trans* dephosphorylation by other molecules of the same species; we believe that individual cyt-PTPe molecules can autodephosphorylate in *cis*, although this requires experimental validation. In all, we conclude that cyt-PTPe can down-regulate its own activation of Src, thus providing a mechanism that limits Src activation downstream of integrins.

DISCUSSION

Activation of integrin receptors in osteoclasts activates the Src kinase, which is an essential component in the resulting cellular response. We have shown previously that cyt-PTPe helps activate Src following activation of integrins in osteoclasts. In the absence of cyt-PTPe, Src is not sufficiently activated, the structure and organization of the podosomal adhesion structures of osteoclasts are abnormal, and osteoclast activity is reduced. Phosphorylation of cyt-PTPe at its terminal Tyr-683 is essential for the phosphatase to activate Src. Here we show that GRB2 plays a critical role in this process by bridging between cyt-PTPe and Src. Our studies indicate that GRB2 is required also for events downstream of Src activation, including cyt-PTPe phosphorylation at Tyr-638, proper differentiation of OCLs, and organization of their podosomes. These results do not agree with the phosphodisplacement model for Src activation in which the C-terminal phosphotyrosine of a PTP directly binds the SH2 domain of Src. This model suggests that Src undergoes inhibition, not activation, by GRB2.

Mechanistically we show that GRB2 associates with Src using its N-terminal SH3 and SH2 domains. Both domains participate in this association because either isolated domain can bind Src (Fig. 5*A*) and because full-length GRB2 in which either one of these domains was inactivated remained able to bind Src (Fig. 5*B*). Further studies are required to identify the sites in Src to which GRB2 binds and to determine how this association helps PTPe to activate Src. The Src-GRB2 association does not require the presence of cyt-PTPe and occurs independently of it (Fig. 5*C*). Conversely, the association between GRB2 and cyt-PTPe is dependent on Tyr(P)-638 of cyt-PTPe binding the GRB2 SH2 domain (Ref. 31 and Figs. 1 and 5, *A* and *B*); phosphorylation of cyt-PTPe and its association with GRB2 were induced by activation of osteoclast integrins (Fig. 4*C*). The existence of a cyt-PTPe-GRB2-Src signaling axis is strongly supported by the finding that cyt-PTPe required the presence of GRB2 to rescue activation of Src in EKO OCLs (Fig. 3*C*).

A model that summarizes our findings is shown in Fig. 9. The SH2 domain of GRB2 binds both cyt-PTPe and Src, suggesting that these molecules cannot be bridged by a single GRB2 molecule that contains one SH2 domain (Fig. 9*A*). It is thus possible that a dimer or higher order association of GRB2 mediates this association; the data do not exclude the possibility that the GRB2-GRB2 interactions are indirect, using another molecule to bridge the two GRB2 molecules. We note that GRB2 has been suggested to form dimers that can link the C termini of two FGF2 receptor molecules (34). An alternative model (Fig. 9*B*) is

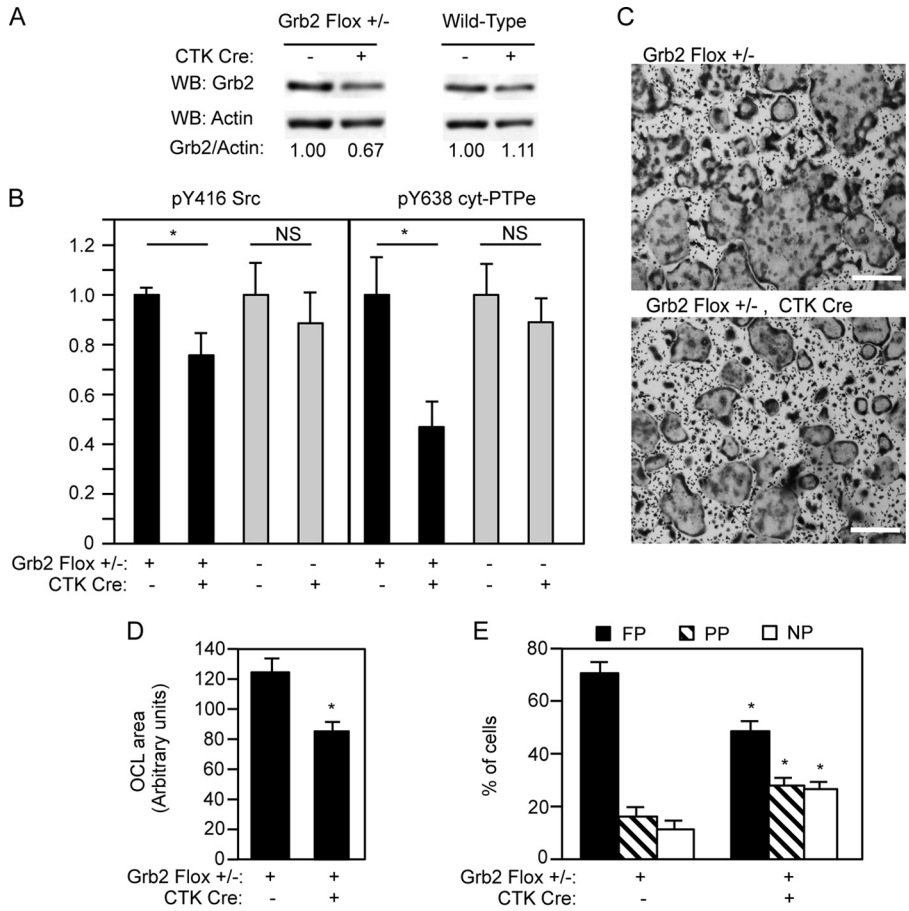

FIGURE 7. **Inactivation of one *Grb2* allele in primary OCLs disrupts cell growth and podosomal organization.** OCLs were prepared from mice heterozygous for a floxed allele of *Grb2* (*Grb2* Flox+/−) or from WT mice that either do or do not express cathepsin K-Cre (*CTK Cre*). *A*, representative blot showing that cathepsin K-Cre expression reduces GRB2 protein levels in OCLs that contain one floxed *Grb2* allele but not in OCLs that contain two wild-type, non-floxed alleles. *B*, reduced GRB2 expression correlates with reduced levels of Tyr(P)-416 Src and Tyr(P)-638 cyt-PTPe following Cre-mediated inactivation of one *Grb2* allele (*black bars*) but not when cathepsin K-Cre alone is expressed (*gray bars*). Shown are mean ± S.E. of $n = 3$–7 repeats per bar. *, $p \leq 0.041$; *NS*, not significant. *C*, pictures of growing OCLs carrying two or one intact *Grb2* alleles stained for tartrate-resistant acid phosphatase. *Scale bars*, 200 μm. *D*, bar diagram showing reduced area covered by OCLs lacking one allele of *Grb2*. *, $p = 0.000234$, 9–15 fields from two to three individual mice per genotype, representative of two experiments. *E*, percentage of OCLs carrying one or two functional *Grb2* alleles whose podosomes are organized in SZLs (fully polarized (*FP*)), in small rings or associations (partially polarized (*PP*)), or at random (non-polarized (*NP*)). *, $p < 0.00135$ for corresponding bars between genotypes. 153–330 cells were analyzed per genotype/treatment. *WB*, Western blot. *Error bars* represent S.E.

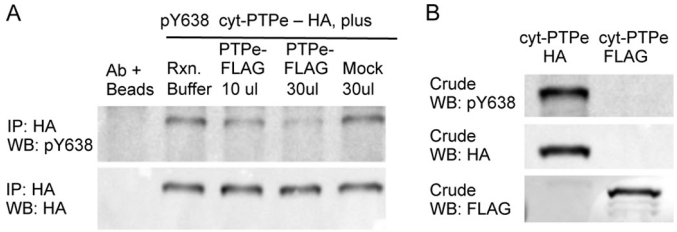

FIGURE 8. ***trans* dephosphorylation at Tyr(P)-638 among cyt-PTPe molecules.** Inactive, HA-tagged Tyr(P)-638 cyt-PTPe was incubated for 30 min at 37 °C with varying amounts of active, non-phosphorylated FLAG-tagged cyt-PTPe. *Left*, increasing amounts of FLAG-cyt-PTPe reduces the amount of phosphorylated HA-cyt-PTPe. *Rxn. Buffer* and *Mock*, incubation of HA-cyt-PTPe with reaction buffer alone or with eluate from beads carrying FLAG antibodies incubated with lysates of mock-transfected 293T cells, respectively. *Ab*, antibody; *WB*, Western blot; *IP*, immunoprecipitation. *Right*, expression and phosphorylation at Tyr-638 of HA-cyt-PTPe and FLAG-cyt-PTPe.

based on our finding that GRB2 can bind Src via either of its SH2 or N-SH3 domains. It is possible that a single GRB2 molecule binds cyt-PTPe via its SH2 domain and Src via its N-SH3 domain. Although we cannot formally rule out this model, we consider it less likely because the isolated SH2 and N-SH3 domains of GRB2 appear to bind Src less well that the entire GRB2 molecule (Fig. 5*A*), suggesting that both domains may be required for optimal binding to Src. Although Src collaborates closely with Pyk2 downstream of activated integrins in OCLs, prior studies indicate that Src, not Pyk2, phosphorylates cyt-PTPe following integrin activation (9). Data shown here indicate that Pyk2 is part of the GRB2·Src complex (Figs. 4*A* and 5*C*) and that GRB2 is required also for activation of Pyk2 (Figs. 2*A* and 3*B*).

The chain of events downstream of activated integrins suggests that activation of Src depends on phosphorylation of cyt-PTPe, which in turn is performed by already active Src. This apparent contradiction is resolved if one considers populations of molecules rather than individual ones. Some Src molecules may be activated following integrin stimulation in a mechanism independent of cyt-PTPe, for example by direct association of the β3 integrin chain with the SH3 domain of Src (35, 36). Active Src molecules phosphorylate cyt-PTPe at Tyr-638, which then recruits additional Src molecules via a GRB2-dependent mechanism and activates them by dephosphorylation

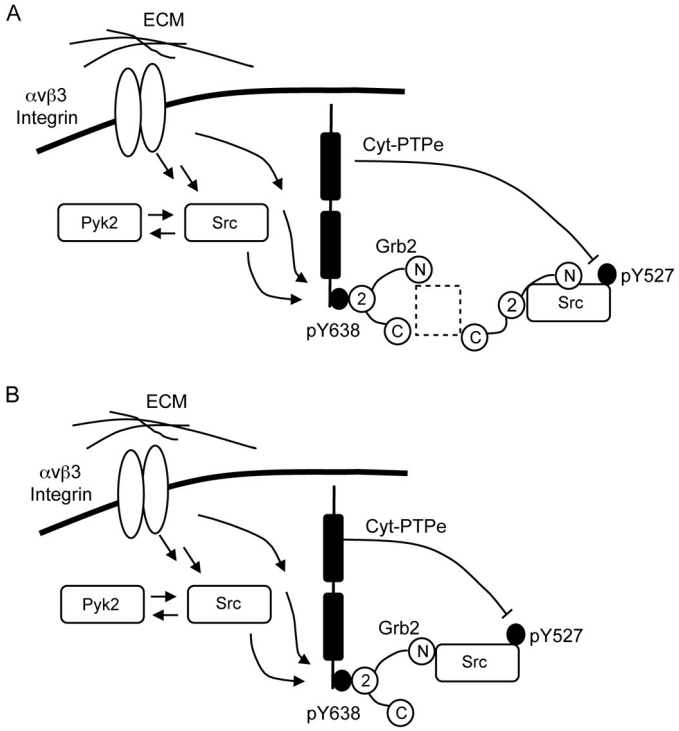

FIGURE 9. **Models depicting possible role of GRB2 in activation of Src by cyt-PTPe in OCLs.** *A*, following activation of αvβ3 integrins in OCLs by physical contact with extracellular matrix (*ECM*), Src is partially activated. cyt-PTPe is phosphorylated at Tyr-638 by the partially active Src or by other kinases. Tyr(P)-638 cyt-PTPe then binds the SH2 domain of GRB2, which recruits (directly or indirectly) a molecule of GRB2 bound to Src. Cyt-PTPe then dephosphorylates Src at Tyr-527, thus activating the kinase. *B*, similar to *A* except that one molecule of GRB2 binds Tyr(P)-638 cyt-PTPe via its SH2 domain and Src via its N-SH3 domain. *2*, *C*, and *N*, SH2, C-terminal SH3, and N-terminal SH3 domains of GRB2, respectively.

at their inhibitory Tyr(P)-527. A positive feedback cycle ensues and ensures full activation of Src and complete phosphorylation of cyt-PTPe at Tyr-638.

Reduction of GRB2 expression in OCLs by half relative to its WT levels using shRNA or targeted gene disruption significantly altered phosphorylation of cyt-PTPe, Src activation and signaling in OCLs, OCL growth, and podosomal organization (Figs. 6 and 7). Most of these effects occur also as the result of elimination of cyt-PTPe expression in OCLs (8, 9). Although our results indicate that GRB2 plays a significant role in mediating activation of Src by cyt-PTPe, the strong effect of removal of a single allele of *Grb2* and the finding that loss of cyt-PTPe and loss of GRB2 affect podosomal organization additively (Fig. 6*D*) indicate that GRB2 affects cytoskeletal organization in OCLs also by additional, cyt-PTPe-independent pathways. This conclusion is further supported by the observation that knock-out of PTPe affected the structure and function of OCLs but not their differentiation. In contrast, reducing GRB2 expression by shRNA or by gene targeting also slowed down OCL differentiation. This finding is not surprising in light of the central roles GRB2 plays in many key signaling pathways.

As indicated, C-terminal phosphorylation of RPTPe and cyt-PTPe is critical for both isoforms to fulfill several of their key functions. Moreover, several PTPs, such as GLEPP1 and DEP1, include C-terminal tyrosine residues embedded in sequence motifs that agree with the consensus for binding the GRB2 SH2 domain. It is therefore possible that C-terminal phosphorylation followed by GRB2 binding is more widespread than described here and helps regulate physiological functions of other PTPs as well.

Acknowledgments—We thank Ofira Higfa and Neri Sharabi for expert animal care.

REFERENCES

1. Georgess, D., Machuca-Gayet, I., Blangy, A., and Jurdic, P. (2014) Podosome organization drives osteoclast-mediated bone resorption. *Cell Adh. Migr.* **8,** 191–204
2. Boyle, W. J., Simonet, W. S., and Lacey, D. L. (2003) Osteoclast differentiation and activation. *Nature* **423,** 337–342
3. Bruzzaniti, A., and Baron, R. (2006) Molecular regulation of osteoclast activity. *Rev. Endocr. Metab. Disord.* **7,** 123–139
4. Teitelbaum, S. L. (2007) Osteoclasts: what do they do and how do they do it? *Am. J. Pathol.* **170,** 427–435
5. Luxenburg, C., Addadi, L., and Geiger, B. (2006) The molecular dynamics of osteoclast adhesions. *Eur. J. Cell Biol.* **85,** 203–211
6. Destaing, O., Sanjay, A., Itzstein, C., Horne, W. C., Toomre, D., De Camilli, P., and Baron, R. (2008) The tyrosine kinase activity of c-Src regulates actin dynamics and organization of podosomes in osteoclasts. *Mol. Biol. Cell* **19,** 394–404
7. Teitelbaum, S. L. (2011) The osteoclast and its unique cytoskeleton. *Ann. N.Y. Acad. Sci.* **1240,** 14–17
8. Chiusaroli, R., Knobler, H., Luxenburg, C., Sanjay, A., Granot-Attas, S., Tiran, Z., Miyazaki, T., Harmelin, A., Baron, R., and Elson, A. (2004) Tyrosine phosphatase ϵ is a positive regulator of osteoclast function *in vitro* and *in vivo*. *Mol. Biol. Cell* **15,** 234–244
9. Granot-Attas, S., Luxenburg, C., Finkelshtein, E., and Elson, A. (2009) PTPϵ regulates integrin-mediated podosome stability in osteoclasts by activating Src. *Mol. Biol. Cell* **20,** 4324–4334
10. Gil-Henn, H., and Elson, A. (2003) Tyrosine phosphatase-ϵ activates Src and supports the transformed phenotype of Neu-induced mammary tumor cells. *J. Biol. Chem.* **278,** 15579–15586
11. Berman-Golan, D., and Elson, A. (2007) Neu-mediated phosphorylation of protein tyrosine phosphatase ϵ is critical for activation of Src in mammary tumor cells. *Oncogene* **26,** 7028–7037
12. Rousso-Noori, L., Knobler, H., Levy-Apter, E., Kuperman, Y., Neufeld-Cohen, A., Keshet, Y., Akepati, V. R., Klinghoffer, R. A., Chen, A., and Elson, A. (2011) Protein tyrosine phosphatase ϵ affects body weight by downregulating leptin signaling in a phosphorylation-dependent manner. *Cell Metab.* **13,** 562–572
13. Sines, T., Granot-Attas, S., Weisman-Welcher, S., and Elson, A. (2007) Association of tyrosine phosphatase ϵ with microtubules inhibits phosphatase activity and is regulated by the epidermal growth factor receptor. *Mol. Cell. Biol.* **27,** 7102–7112
14. Zheng, X. M., Resnick, R. J., and Shalloway, D. (2000) A phosphotyrosine displacement mechanism for activation of Src by PTPα. *EMBO J.* **19,** 964–978
15. Su, J., Yang, L. T., and Sap, J. (1996) Association between receptor protein-tyrosine phosphatase RPTPα and the Grb2 adaptor. Dual Src homology (SH) 2/SH3 domain requirement and functional consequences. *J. Biol. Chem.* **271,** 28086–28096
16. Su, J., Batzer, A., and Sap, J. (1994) Receptor tyrosine phosphatase R-PTP-α is tyrosine-phosphorylated and associated with the adaptor protein Grb2. *J. Biol. Chem.* **269,** 18731–18734
17. den Hertog, J., Tracy, S., and Hunter, T. (1994) Phosphorylation of receptor protein-tyrosine phosphatase α on Tyr789, a binding site for the SH3-SH2-SH3 adaptor protein GRB-2 *in vivo*. *EMBO J.* **13,** 3020–3032
18. den Hertog, J., and Hunter, T. (1996) Tight association of GRB2 with receptor protein-tyrosine phosphatase α is mediated by the SH2 and C-terminal SH3 domains. *EMBO J.* **15,** 3016–3027
19. Zheng, X. M., and Shalloway, D. (2001) Two mechanisms activate PTPα during mitosis. *EMBO J.* **20,** 6037–6049

20. Cheng, S. Y., Sun, G., Schlaepfer, D. D., and Pallen, C. J. (2014) Grb2 promotes integrin-induced focal adhesion kinase (FAK) autophosphorylation and directs the phosphorylation of protein tyrosine phosphatase α by the Src-FAK kinase complex. *Mol. Cell. Biol.* **34,** 348–361
21. Sun, G., Cheng, S. Y., Chen, M., Lim, C. J., and Pallen, C. J. (2012) Protein tyrosine phosphatase α phosphotyrosyl-789 binds BCAR3 to position Cas for activation at integrin-mediated focal adhesions. *Mol. Cell. Biol.* **32,** 3776–3789
22. Elson, A., and Leder, P. (1995) Protein-tyrosine phosphatase ϵ. An isoform specifically expressed in mouse mammary tumors initiated by v-Ha-ras or neu. *J. Biol. Chem.* **270,** 26116–26122
23. Huang, H., Li, L., Wu, C., Schibli, D., Colwill, K., Ma, S., Li, C., Roy, P., Ho, K., Songyang, Z., Pawson, T., Gao, Y., and Li, S. S. (2008) Defining the specificity space of the human SRC homology 2 domain. *Mol. Cell. Proteomics* **7,** 768–784
24. Espejo, A., Côté, J., Bednarek, A., Richard, S., and Bedford, M. T. (2002) A protein-domain microarray identifies novel protein-protein interactions. *Biochem. J.* **367,** 697–702
25. Peretz, A., Gil-Henn, H., Sobko, A., Shinder, V., Attali, B., and Elson, A. (2000) Hypomyelination and increased activity of voltage-gated K^+ channels in mice lacking protein tyrosine phosphatase ϵ. *EMBO J.* **19,** 4036–4045
26. Bisson, N., Ruston, J., Jeansson, M., Vanderlaan, R., Hardy, W. R., Du, J., Hussein, S. M., Coward, R. J., Quaggin, S. E., and Pawson, T. (2012) The adaptor protein Grb2 is not essential for the establishment of the glomerular filtration barrier. *PLoS One* **7,** e50996
27. Nakamura, T., Imai, Y., Matsumoto, T., Sato, S., Takeuchi, K., Igarashi, K., Harada, Y., Azuma, Y., Krust, A., Yamamoto, Y., Nishina, H., Takeda, S., Takayanagi, H., Metzger, D., Kanno, J., Takaoka, K., Martin, T. J., Chambon, P., and Kato, S. (2007) Estrogen prevents bone loss via estrogen receptor α and induction of Fas ligand in osteoclasts. *Cell* **130,** 811–823
28. Chen, C. A., and Okayama, H. (1988) Calcium phosphate-mediated gene transfer: a highly efficient transfection system for stably transforming cells with plasmid DNA. *BioTechniques* **6,** 632–638
29. Tiscornia, G., Singer, O., and Verma, I. M. (2006) Production and purification of lentiviral vectors. *Nat. Protoc.* **1,** 241–245
30. Finkelshtein, E., Lotinun, S., Levy-Apter, E., Arman, E., den Hertog, J., Baron, R., and Elson, A. (2014) Protein tyrosine phosphatases ϵ and α perform nonredundant roles in osteoclasts. *Mol. Biol. Cell* **25,** 1808–1818
31. Toledano-Katchalski, H., and Elson, A. (1999) The transmembranal and cytoplasmic forms of protein tyrosine phosphatase ϵ physically associate with the adaptor molecule Grb2. *Oncogene* **18,** 5024–5031
32. Lowenstein, E. J., Daly, R. J., Batzer, A. G., Li, W., Margolis, B., Lammers, R., Ullrich, A., Skolnik, E. Y., Bar-Sagi, D., and Schlessinger, J. (1992) The SH2 and SH3 domain-containing protein GRB2 links receptor tyrosine kinases to ras signaling. *Cell* **70,** 431–442
33. Clark, S. G., Stern, M. J., and Horvitz, H. R. (1992) *C. elegans* cell-signalling gene *sem-5* encodes a protein with SH2 and SH3 domains. *Nature* **356,** 340–344
34. Lin, C. C., Melo, F. A., Ghosh, R., Suen, K. M., Stagg, L. J., Kirkpatrick, J., Arold, S. T., Ahmed, Z., and Ladbury, J. E. (2012) Inhibition of basal FGF receptor signaling by dimeric Grb2. *Cell* **149,** 1514–1524
35. Arias-Salgado, E. G., Lizano, S., Sarkar, S., Brugge, J. S., Ginsberg, M. H., and Shattil, S. J. (2003) Src kinase activation by direct interaction with the integrin β cytoplasmic domain. *Proc. Natl. Acad. Sci. U.S.A.* **100,** 13298–13302
36. Obergfell, A., Eto, K., Mocsai, A., Buensuceso, C., Moores, S. L., Brugge, J. S., Lowell, C. A., and Shattil, S. J. (2002) Coordinate interactions of Csk, Src, and Syk kinases with αIIbβ3 initiate integrin signaling to the cytoskeleton. *J. Cell Biol.* **157,** 265–275